Electronic Supplementary Information

Mesoporous hydrogel electrodes with flexible framework exhibiting enhanced mass transport for oxygen evolution reaction

Ritsuki Nakajima,[a] Hiroki Wago,[a] Tatsuya Taniguchi,[b] Yuta Sasaki,[b] Yoshinori Nishiki,[c] Zaenal Awaludin,[c] Takaaki Nakai,[c] Akihiro Kato,[c] Shigenori Mitsushima[a,d], and Yoshiyuki Kuroda[*a,d]

[a.] Department of Chemistry Applications and Life Science, Graduate School of Engineering Science, Yokohama National University, 79-5 Tokiwadai, Hodogaya-ku, Yokohama Kanagawa 240-8501, Japan

[b.] Kawasaki Heavy Industries Ltd., 1-1 Kawasaki-cho, Akashi, Hyogo 673-8666, Japan

[c.] De Nora Permelec Ltd., 2023-15 Endo, Fujisawa, Kanagawa 252-0816, Japan

[d.] Advanced Chemical Energy Research Center, Institute of Advanced Sciences, Yokohama National University, 79-5 Tokiwadai, Hodogaya-ku, Yokohama Kanagawa 240-8501, Japan

Experimental section

Materials

Cobalt chloride hexahydrate ($CoCl_2 \cdot 6H_2O$, 99.0%), cobalt nitrate hexahydrate ($Co(NO_3)_2 \cdot 6H_2O$, 98.0%), and a standard solution of cobalt for ICP-AES (1000 ppm of Co, 0.1 M HNO_3) were purchased from Kanto Chemical Co. Inc. Tris-NH_2 (99.0%), hydrochloric acid (HCl, 35.0~37.0%), 1-butanol (99.0%), and aqueous ammonia (28.0~30.0%) were purchased from FUJIFILM Wako Pure Chemical Co. Pluronic F127 was purchased from Sigma–Aldrich. Potassium hydroxide (KOH, 85.0%) was purchased from Junsei Chemicals Co., Ltd. The Ni plate was purchased from Kouei Co., Ltd. The Ni wire was purchased from Nilaco Co. The Ni plate and wire were etched in boiling 6 M HCl to remove the oxide layer from the surface. All the other chemicals were used as received, without further purification.

Synthesis of hybrid cobalt hydroxide nanosheet (Co-ns)

An aqueous solution of 0.1 M $CoCl_2 \cdot 6H_2O$ (100 mL) was poured into an aqueous solution of 1.0 M Tris-NH_2 (100 mL) and heated at 80 °C for 24 h. The product was filtered through a membrane filter (pore size: 0.2 μm). The gel obtained was washed with deionized water and filtered twice. The gel was re-dispersed in water to a concentration of 50 $mg \cdot mL^{-1}$ and exfoliated via sonication.

Preparation of mesoporous hydrogel electrodes

A three-electrode cell made of perfluoroalkoxy alkane (PFA) was used for the electrochemical deposition of mesoporous hydrogel electrodes from the Co-ns. A Ni plate (0.5 × 0.5 cm^2), a Ni coil, and an RHE were used as working, counter, and reference electrodes, respectively. An aqueous solution of 1 M KOH was used as the electrolyte at 30 °C under stirring at 600 rpm. A dispersion of Co-ns was added to the electrolyte to adjust the concentration of Co-ns to 40 ppm. Co-ns were electrochemically deposited on the Ni plate via constant-current electrolysis at 800 $mA \cdot cm^{-2}$. The electrolysis duration was varied from 0.5 to 30 h to control the thickness.

Preparation of rigid mesoporous electrodes

12.4 g of $Co(NO_3)_2 \cdot 6H_2O$ and 5.0 g of Pluronic F127 were dissolved in 50 mL of 1-butanol to prepare a precursor solution. A Ni plate was immersed in the precursor solution and dip-coated at a lifting rate of 0.2 $cm \cdot s^{-1}$, dried at 80 °C for 20 min, heated at 400 °C for 30 min, and cooled at room temperature. This cycle was repeated 6–70 times to control the thickness. Finally, the electrode was heated at 400 °C for 30 min.

Preparation of conventional porous CoOOH film

Aqueous ammonia was added to an aqueous solution of 0.1 M $CoCl_2$ to adjust the pH to 12. A Ni substrate etched in 6 M HCl for 6 min was immersed in the solution to serve as the working electrode. A Ni coil and a Ag/AgCl reference electrode were used as the counter and reference electrodes, respectively. The deposition of CoOOH was performed via 30 cycles of CV in the potential range of 0–1.2 V vs. saturated calomel electrode at a scan rate of 20 $mV \cdot s^{-1}$.

Electrochemical measurements

The same electrochemical cell was used to prepare the mesoporous hydrogel electrodes. Mesoporous hydrogel and rigid mesoporous electrodes were used as the working electrodes. A Ni coil and an RHE were used as the counter and reference electrodes, respectively. An aqueous solution of 1 M KOH was used as the electrolyte at 30 °C.

CV was performed at a scan rate of 50 $mV \cdot s^{-1}$ in the potential range of 0.5–1.6 V vs. RHE for three cycles to analyze the redox reactions of Co in the catalysts. CV was performed at a scan rate of 5 $mV \cdot s^{-1}$ in the potential range of 0.5–1.8 V vs. RHE for two cycles to analyze the OER performance. Electrochemical impedance spectroscopy was used to determine the solution resistance by analyzing the high-frequency intercept. Bias current density and current amplitude were 50 and 15 $mA \cdot cm^{-2}$, respectively. AC frequency was scanned from 10^0 Hz to 10^5 Hz. The obtained data were analyzed, using the dedicated software EC-lab software V11.33 (Bio-Logic –

Science Instruments). The Nyquist plots were fitted by the following Rundles-type equivalent circuit to determine the high-frequency resistance (R_s).

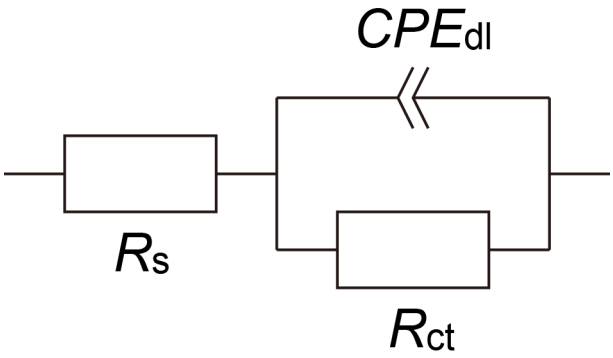

The *iR* drop of the cyclic voltammograms were corrected using the high-frequency resistance.

Characterization

XRD patterns were collected using a Rigaku Ultima IV diffractometer with CuKα radiation at 40 kV and 40 mA. The powdery samples were mounted on a Si non-reflecting sample plate. FTIR spectra were obtained using a JASCO FT/IR6100 spectrometer with a KBr disk. The peak resolution was set to 4.0 cm^{-1}. Elemental analysis was performed using ICP-AES with an SII SPS3000 spectrometer. To prepare sample solutions, an electrode coated with the catalyst is immersed in 50 μL of 18% HCl aq. (analysis grade) to dissolve the cobalt-based catalyst in the solution while heating at approximately 80 °C. Deionized water was added to the solution if there was remaining solid materials except for the nickel substrate. The solution was then transferred to a 25 mL volumetric flask and the volume was made up to 100 mL with deionized water. The 1000 ppm standard solution of Co was diluted to prepare those with the concentration of 0, 0.5, 2.0, 5.0, 10, 20, 30, and 50 ppm, containing 0.1 M HNO_3 (analysis grade). The emission of Co at 228.6 nm was used for the quantification of Co in the samples, at which wavelength no other emission interferes (e.g., Ni and K). The TG curves were recorded using a Rigaku Thermo Plus EVO2 instrument. Samples were placed on an Al pan (φ5 mm). Temperature was raised from 30 °C to 150 °C at the ramp rate of 10 °C·min^{-1}, and kept at 150 °C for 60 min under dry air flow. XRF spectra were obtained using a JEOL JSX-3100RII spectrometer at 30 kV and 1 mA. The collimator diameter was 1 mm. The amount of Co deposited on the film was evaluated using the

fundamental parameter method. CLSM images were recorded using a KEYENCE VK-X200 microscope, equipped with a violet laser (λ = 408 nm). ×20 magnification was used for the analyses. FE-SEM images were recorded using a Hitachi SU8020 microscope without a metal coating, at the accelerating voltage of 30 kV and the emission current of 20 μA. The solvent in the hydrogel samples was sequentially replaced with deionized water and ethanol before drying.

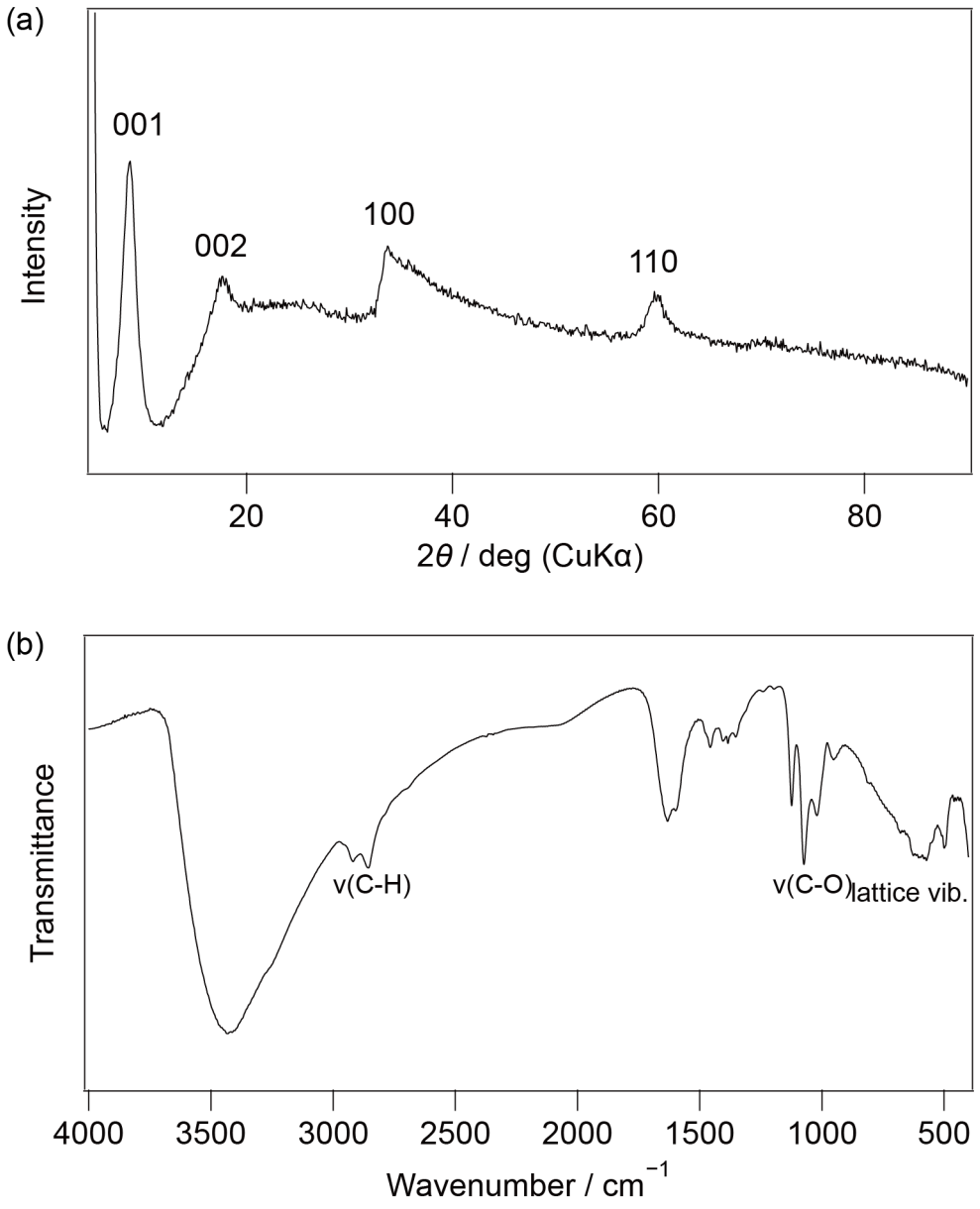

Fig. S1 (a) XRD pattern and (b) FTIR spectrum of Co-ns. Reprinted with permission from R. Nakajima, T. Taniguchi, Y. Sasaki, Y. Nishiki, Z. Awaludin, T. Nakai, A. Kato, S. Mitsushima, Y. Kuroda, *ChemSusChem*, **2023**, e202300384. Copyright 2023 Wiley-VCH.

The background of (a) is affected by the fluorescent X-ray of cobalt due to irradiation of CuKα X-ray. The asymmetric 100 diffraction is caused by the random stacking of nanosheets. Please see the reference 15 for detail.

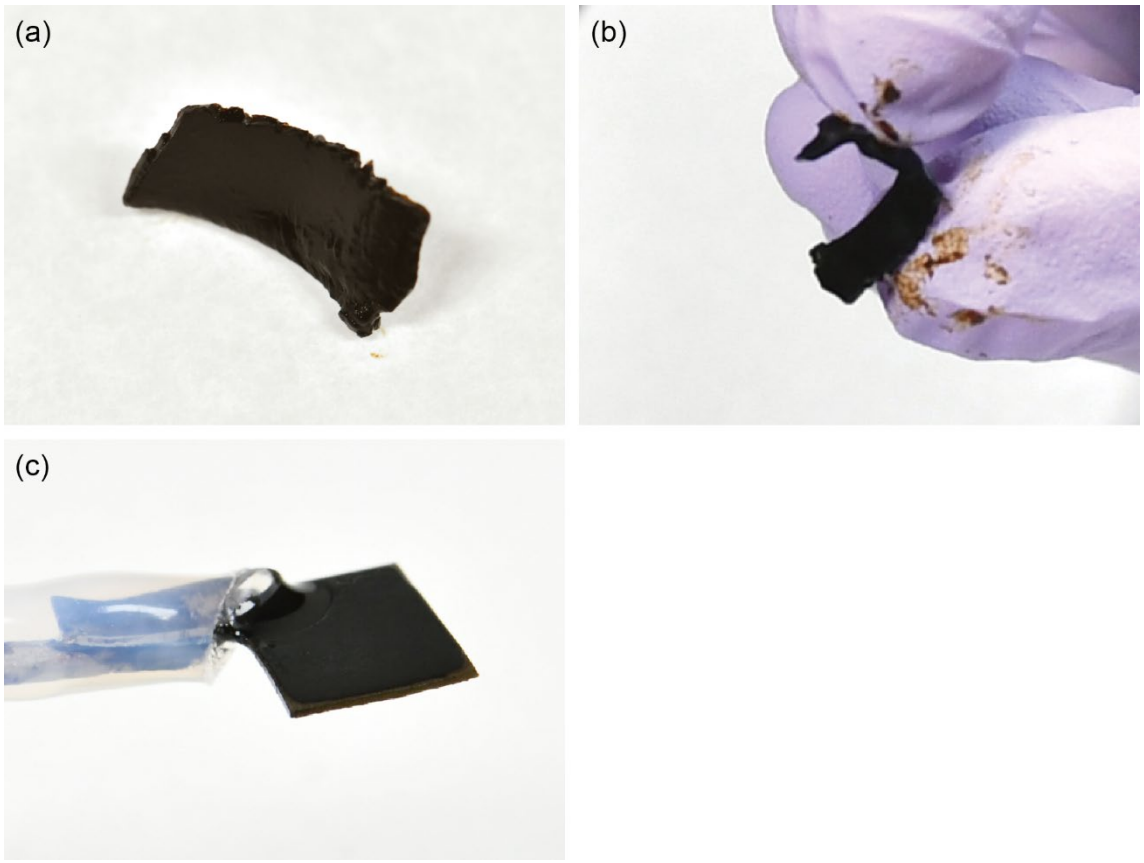

Fig. S2 Photographs of (a) the hydrogel of Co-ns, (b) the bent hydrogel of Co-ns, and (c) MHG-9 formed on a Ni plate.

Fig. S3 Photograph of the colloidal dispersion of Co-ns. A green laser was used to show the Tyndall effect.

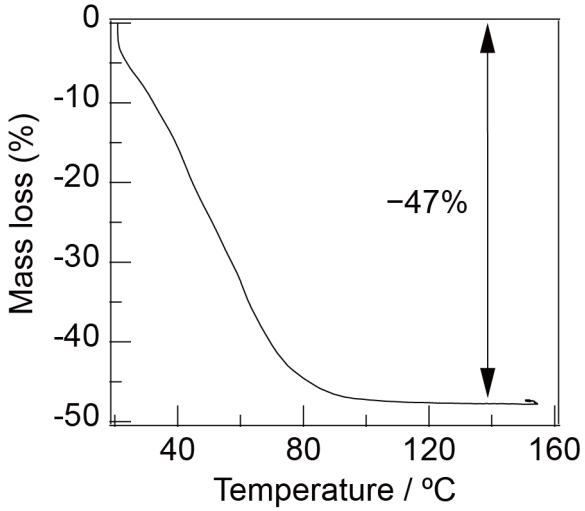

Fig. S4 TG curve of the Co-ns gel.

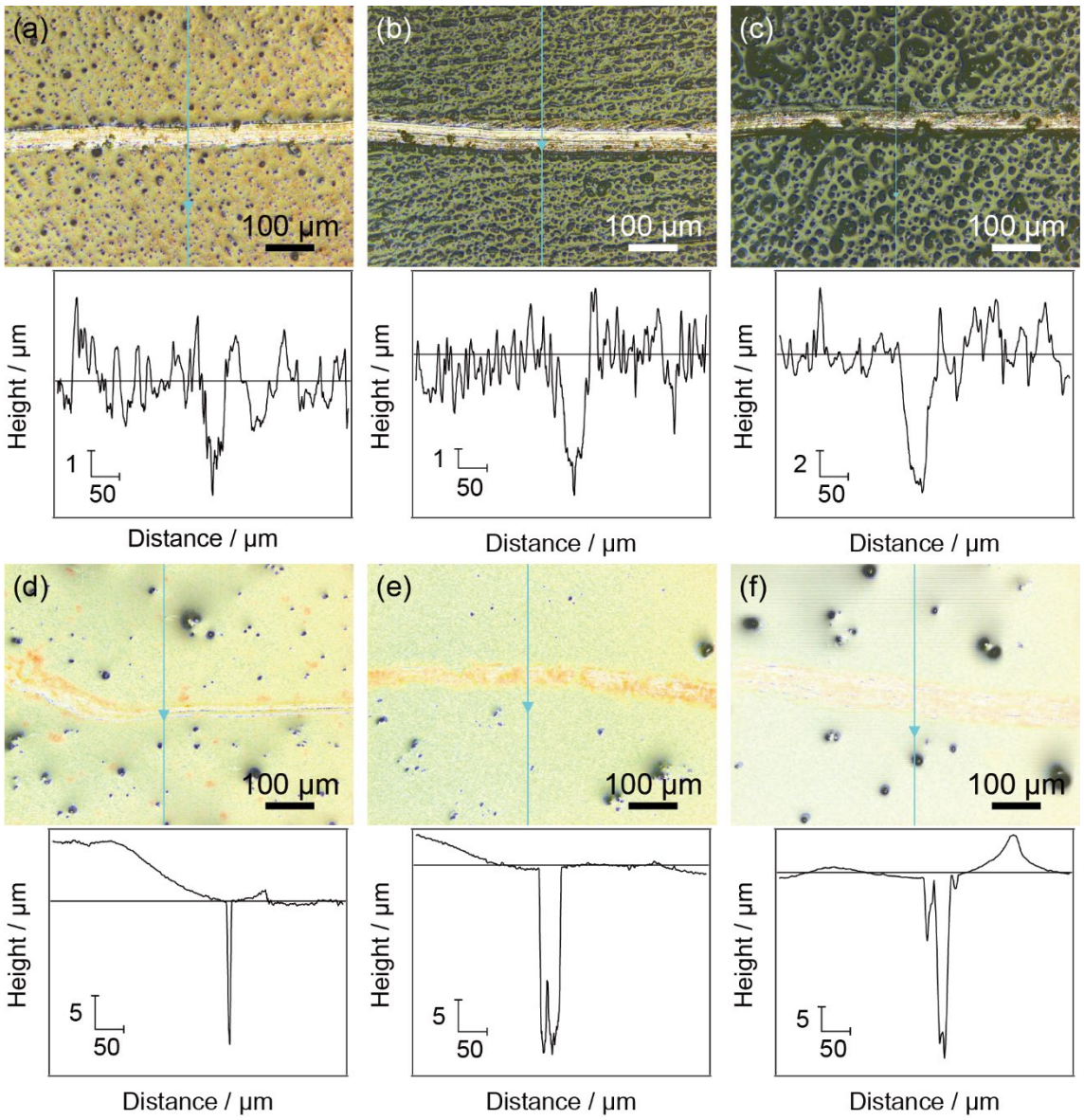

Fig. S5 CLSM images and the corresponding height profiles around scratches of (a) MHG-4, (b) MHG-6, (c) MHG-9, (d) MHG-20, (e) MHG-27, and (f) MHG-37.

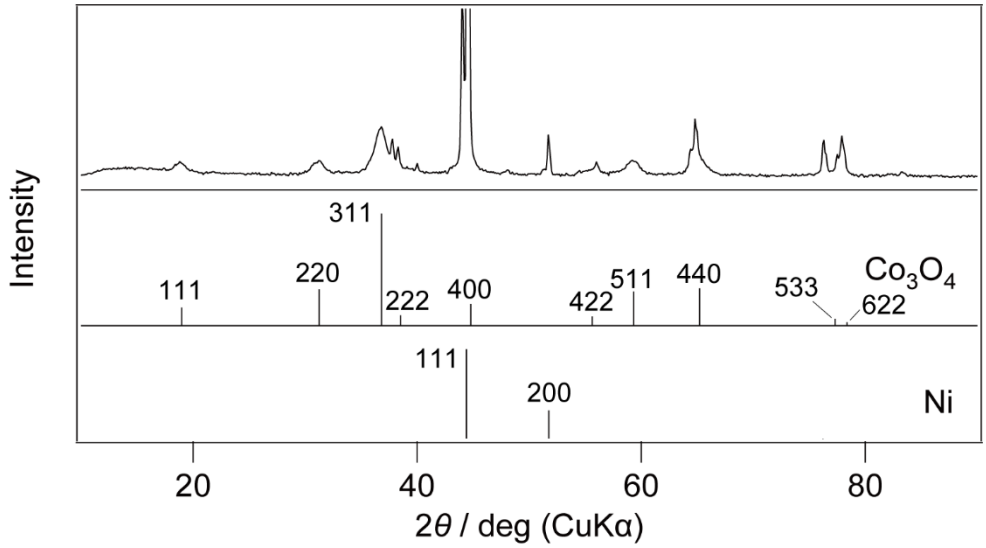

Fig. S6 XRD pattern of RMP-60 and the standard patterns of Co_3O_4 and Ni. The XRD patterns of the other rigid mesoporous electrodes are essentially identical.

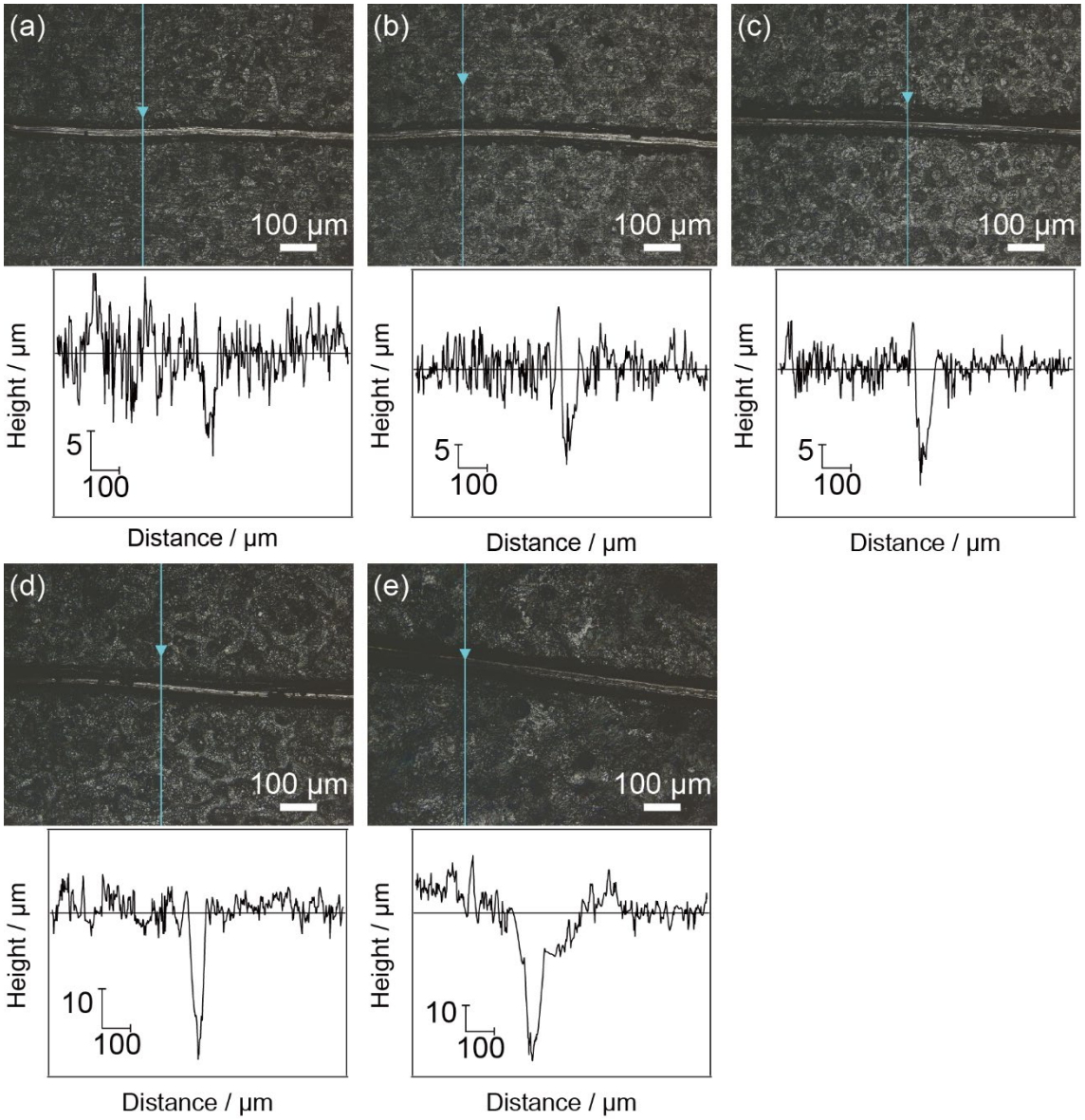

Fig. S7 CLSM images and the corresponding height profiles of (a) RMP-10, (b) RMP-15, (c) RMP-20, (d) RMP-35, and (e) RMP-60.

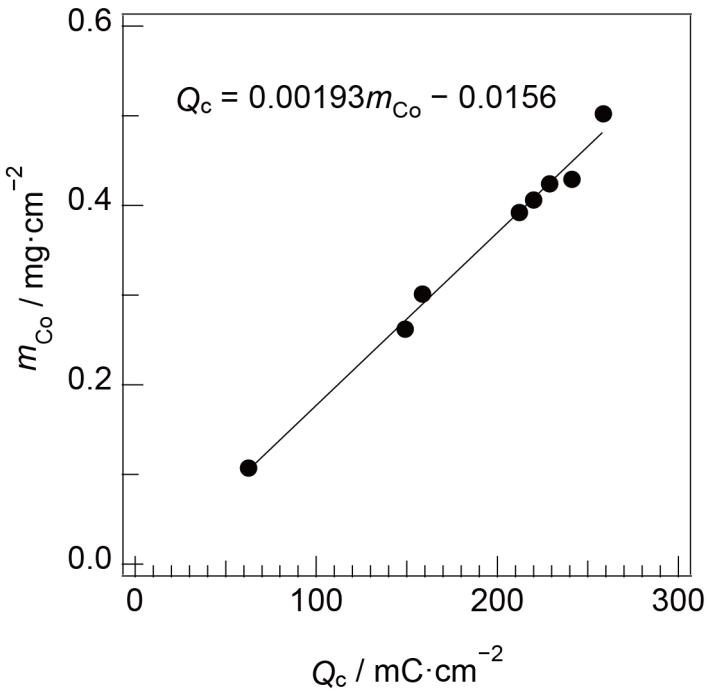

Fig. S8 Standard curve of the deposited amount of Co (m_{Co}) with respect to the charge density of Co (Q_c).

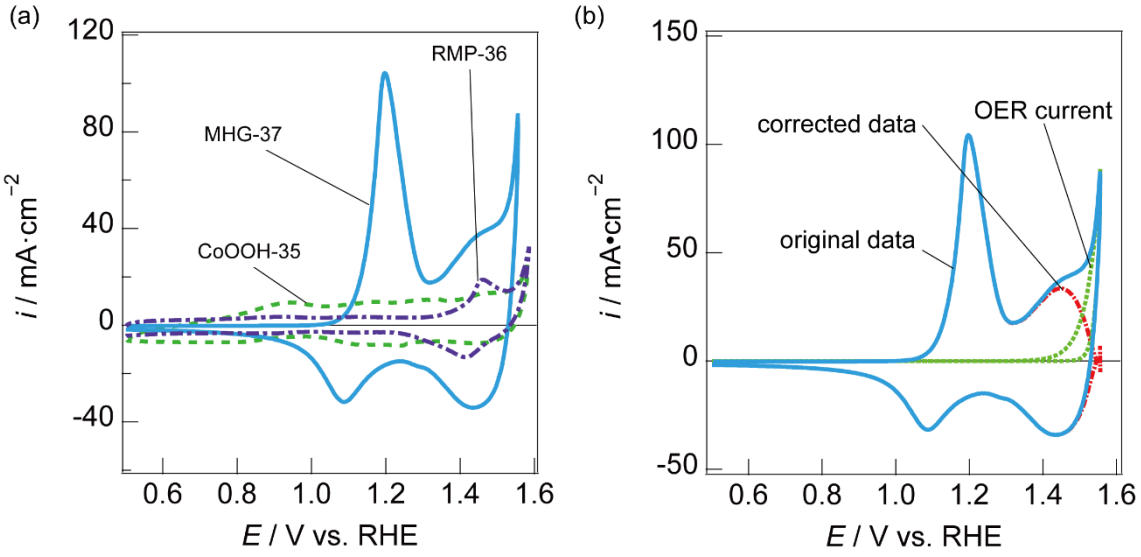

Fig. S9 (a) Cyclic voltammograms of MHG-37, RMP-36, and CoOOH-35 without the correction of the OER current. (b) Cyclic voltammogram of MHG-37 decomposed into the OER current and the OER-corrected data.

The OER currents in the cyclic voltammograms were corrected as follows. The polarization curve at potentials higher than 1.55 V vs. RHE was assumed to be the OER current, which follows the Tafel equation. Thus, the region was fitted with the Tafel equation $\eta = a + b \log i$. After the parameters a and b were determined, the Tafel curve was extrapolated to the entire potential region (Fig. S10b, OER current). OER-corrected data were obtained by subtracting the OER current from the original data.

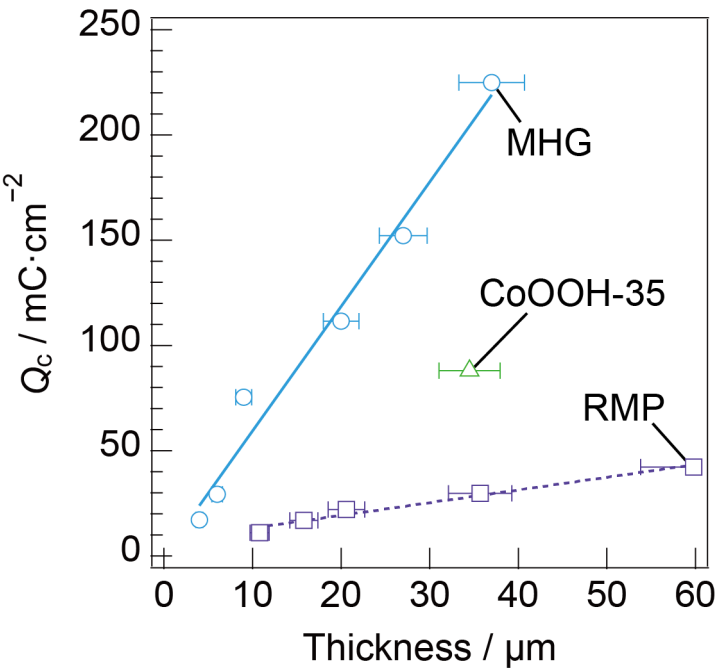

Fig. S10 Redox charge of Co with respect to the film thickness. Error bars indicate 95% confidence intervals.

Table S1 Linear fit equation and the coefficient of determination of the relationship between the current density at a predefined potential and the film thickness.

	$i_{1.55}$		$i_{1.60}$	
	linear fit equation	R^2	linear fit equation	R^2
MHG-37	y=1.69x–2.04	0.980	y=8.11x–31.41	0.935
RMP-36	y=0.14x–1.55	0.840	y=0.30x–23.38	0.669